Flavoenzyme-mediated Regioselective Aromatic Hydroxylation with Coenzyme Biomimetics

Guarneri, Alice; Westphal, Adrie H.; Leertouwer, Jos; Lunsonga, Joy; Franssen, Maurice C.R.; Opperman, Diederik J.; Hollmann, Frank; van Berkel, Willem J.H.; Paul, Caroline E.

DOI
10.1002/cctc.201902044

Publication date
2020

Document Version
Final published version

Published in
ChemCatChem

ChemPubSoc Europe

DOI: 10.1002/cctc.201902044

CHEMCATCHEM Full Papers

Flavoenzyme-mediated Regioselective Aromatic Hydroxylation with Coenzyme Biomimetics

Alice Guarneri,[a] Adrie H. Westphal,[b] Jos Leertouwer,[c] Joy Lunsonga,[a] Maurice C. R. Franssen,[a] Diederik J. Opperman,[d] Frank Hollmann,[c] Willem J. H. van Berkel,[e] and Caroline E. Paul*[c]

Regioselective aromatic hydroxylation is desirable for the production of valuable compounds. External flavin-containing monooxygenases activate and selectively incorporate an oxygen atom in phenolic compounds through flavin reduction by the nicotinamide adenine dinucleotide coenzyme, and subsequent reaction with molecular oxygen. This study provides the proof of principle of flavoenzyme-catalyzed selective aromatic hydroxylation with coenzyme biomimetics. The carbamoylmethyl-substituted biomimetic in particular affords full conversion in less than two hours for the selective hydroxylation of 5 mM 3- and 4-hydroxybenzoates, displaying similar rates as with NADH, achieving a 10 mM/h enzymatic conversion of the medicinal product gentisate. This biomimetic appears to generate less uncoupling of hydroxylation that typically leads to undesired hydrogen peroxide. Therefore, we show these flavoenzymes have the potential to be applied in combination with biomimetics.

Introduction

The regioselective oxidation of aromatic C–H bonds is of high interest in organic synthesis to produce valuable compounds for the fine chemical and pharmaceutical industry. However, this reaction is still challenging due to a lack of efficiency and selectivity with traditional catalysts.[1] Alternatively, enzymes such as heme-containing peroxygenases and monooxygenases hydroxylate a wide range of aromatic compounds efficiently, yet with limited regioselectivity.[2] Flavin-containing hydroxylases, on the other hand, are less 'promiscuous' but display exquisite regioselectivity for the hydroxylation of anilines, phenols and pyridines.[3] These monooxygenases activate molecular oxygen through transient formation of a flavin C4a-hydroperoxide and subsequent insertion of one oxygen atom into the substrate.[4] From a chemical synthesis perspective, flavin-containing hydroxylases are attractive catalysts, generating aromatic products that display anti-cancer, anti-inflammatory or anti-microbial properties.[5]

Hydroxylases that harbor a tightly bound flavin adenine dinucleotide (FAD) are classified as group A flavoprotein monooxygenases.[3c,6] These enzymes share a similar fold and use nicotinamide adenine dinucleotide (phosphate) in its reduced form (NAD(P)H, Figure 1) as an electron donor to reduce the flavin prosthetic group (Figure 2).[6] Some group A members are highly specific for NADPH or for NADH, whereas

[a] A. Guarneri, J. Lunsonga, Dr. M. C. R. Franssen
Laboratory of Organic Chemistry
Wageningen University
Stippeneng 4
Wageningen 6708 WE (The Netherlands)
[b] A. H. Westphal
Laboratory of Biochemistry
Wageningen University
Stippeneng 4
Wageningen 6708 WE (The Netherlands)
[c] J. Leertouwer, Prof. F. Hollmann, Dr. C. E. Paul
Department of Biotechnology
Delft University of Technology
Van der Maasweg 9
Delft 2629 HZ (The Netherlands)
E-mail: c.e.paul@tudelft.nl
[d] Dr. D. J. Opperman
Department of Biotechnology
University of the Free State
205 Nelson Mandela Drive
Bloemfontein 9300 (South Africa)
[e] Prof. W. J. H. van Berkel
Laboratory of Food Chemistry
Wageningen University
Bornse Weilanden 9
Wageningen 6708 WG (The Netherlands)

Supporting information for this article is available on the WWW under https://doi.org/10.1002/cctc.201902044

This publication is part of a joint Special Collection with ChemBioChem on "Excellence in Biocatalysis Research". Please follow the link for more articles in the collection.

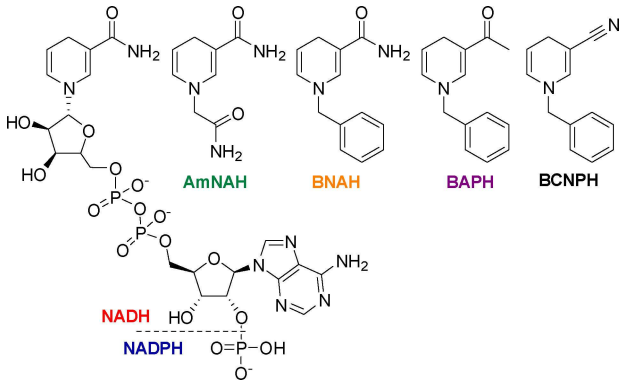

Figure 1. Representative structures of reduced forms of nicotinamide adenine dinucleotide (NADH and NADPH) and coenzyme biomimetics used in this study (AmNAH: 1-(2-carbamoylmethyl)-1,4-dihydronicotinamide, BNAH: 1-benzyl-1,4-dihydronicotinamide, BAPH: 1-benzyl-3-acetyl-1,4-dihydropyridine; BCNPH: 1-benzyl-3-cyano-1,4-dihydropyridine).

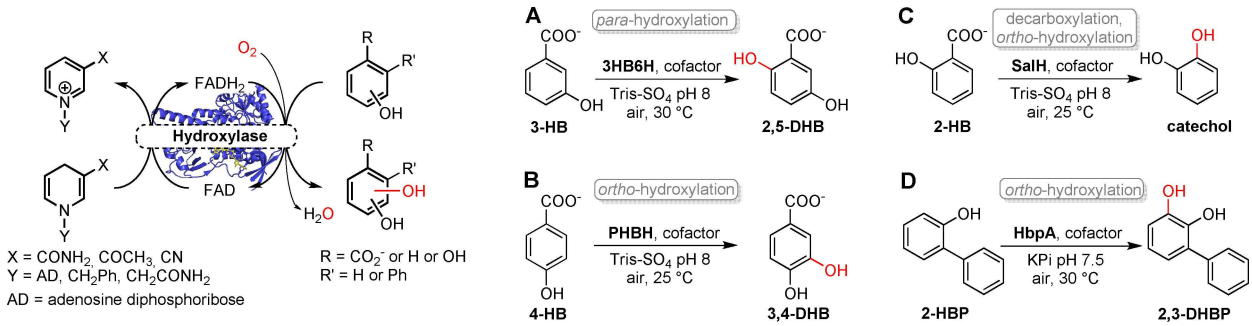

Figure 2. Selective enzymatic aromatic hydroxylation of phenolic substrates: *para*-hydroxylation of 3-hydroxybenzoate (3-HB) to 2,5-dihydroxybenzoate (2,5-DHB) by 3HB6H (**A**); *ortho*-hydroxylation of 4-hydroxybenzoate (4-HB) to 3,4-dihydroxybenzoate (3,4-DHB) by PHBH (**B**); decarboxylation and *ortho*-hydroxylation of 2-hydroxybenzoate (2-HB) to 1,2-dihydroxybenzene (catechol) by SalH (**C**); *ortho*-hydroxylation of 2-hydroxybiphenyl (2-HBP) to 2,3-hydroxybiphenyl (2,3-DHBP) by HbpA (**D**).

others accept both coenzymes with similar efficiency.[7] These hydroxylases lack a Rossmann-type dinucleotide binding domain and the exact way they bind the NAD(P)H coenzyme and trigger the flavin reduction remains unclear.

We became interested to investigate whether flavin-containing monooxygenases of group A accept nicotinamide coenzyme biomimetics (NCBs) to improve their applicability for regioselective aromatic hydroxylation. NCBs are synthetic truncated versions of NAD(P)H with variable substituents (Figure 1).[8] The biocatalytic applications of NCBs were demonstrated with dehydrogenases,[9] ene reductases,[10] azoreductases,[11] cytochrome P450s,[12] NADH oxidases,[10b,13] and two-component flavoprotein monooxygenases (group E and F).[14] NCBs are attractive to study the impact of redox potential and mode of coenzyme binding in oxidoreductases in order to elucidate their mechanism,[10b] and to further apply these enzymes in large scale reactions.[15]

We previously showed the reduction rate of the flavin cofactor varies according to the NCB substituents and redox potential in ene reductases.[10b,16] Additionally, NCBs directly reduce free flavins in solution.[14a] Here we investigate the use of NCBs with group A flavoprotein hydroxylases. For our kinetic and biocatalytic studies, we chose four enzymes:

1) 3-Hydroxybenzoate 6-hydroxylase (3HB6H; EC 1.14.13.24) from *Rhodococcus jostii* RHA1, which catalyzes the *para*-hydroxylation of 3-hydroxybenzoate to 2,5-dihydroxybenzoate (2,5-DHB, gentisate, Figure 2A).[17]
2) *para*-Hydroxybenzoate hydroxylase (PHBH; EC 1.14.13.2) from *Pseudomonas fluorescens*, which catalyzes the *ortho*-hydroxylation of 4-hydroxybenzoate to 3,4-dihydroxybenzoate (3,4-DHB, protocatechuate, Figure 2B).[18]
3) Salicylate hydroxylase (SalH; EC 1.14.13.1) from *Pseudomonas putida*, which catalyzes the oxidative decarboxylation of 2-hydroxybenzoate to 1,2-dihydroxybenzene (catechol, Figure 2C).[19]
4) 2-Hydroxybiphenyl 3-monooxygenase from *Pseudomonas azelaica* HBP1 (HbpA; EC 1.14.13.44),[20] which catalyzes the *ortho*-hydroxylation of 2-hydroxybiphenyl to 2,3-dihydroxybiphenyl (2,3-DHBP, Figure 2D).[20]

3HB6H and PHBH have a stringent substrate specificity,[21] whereas SalH and HbpA are more 'promiscuous'.[22] In addition, we were eager to test group B flavoprotein monooxygenases (Type I Baeyer-Villiger monooxygenases, BVMOs), which also contain a tightly bound FAD cofactor and catalyze valuable Baeyer-Villiger type reactions and sulfoxidations.[23] In this respect, the wild-type cyclohexanone monooxygenase (CHMO) from *Acinetobacter sp.* NCIMB9871, one mutant ($CHMO_{M16}$),[24] and one BVMO from *Aspergillus flavus* ($BVMO_{791}$)[25] were selected.

Results

Catalytic properties of hydroxylases with NCBs

We first compared the time-dependent enzymatic hydroxylation of the native substrates of 3HB6H, PHBH and SalH, using two biomimetics (AmNAH and BNAH) and the two natural coenzymes NADH and NADPH (Figure 3, 4 and 5).

3HB6H fully converted its substrate 3-hydroxybenzoate (3-HB, Figure 2A) into the product gentisate (2,5-DHB) within 30 min with a similar reaction time course, using an excess of NADPH or NADH (Figure 3). The same reaction with AmNAH took 1 h for completion, and with BNAH 1 h 40 min. We screened an additional nitrile-substituted coenzyme, BCNPH (Figure 1), but observed no product formation (Figure S1).

NADH and NADPH promptly solubilized in the reaction mixture, whereas crystallized AmNAH needed *ca.* 20 min to dissolve and BNAH crystals persisted during the reaction. To verify whether the poor water solubility of BNAH affected the rate of the reaction, DMSO was used as co-solvent (concentrations up to 5% v/v of this solvent do not influence the enzyme activity, Figure S4 and S5). Under these conditions, higher initial reaction rates were observed but no difference in conversion was achieved after one hour (Figure S1), which can be in part due to coenzyme oxidation and chemical decomposition over time.[26]

AmNAH was further used for the 3HB6H-catalyzed regioselective hydroxylation of the alternative substrate 3-amino-

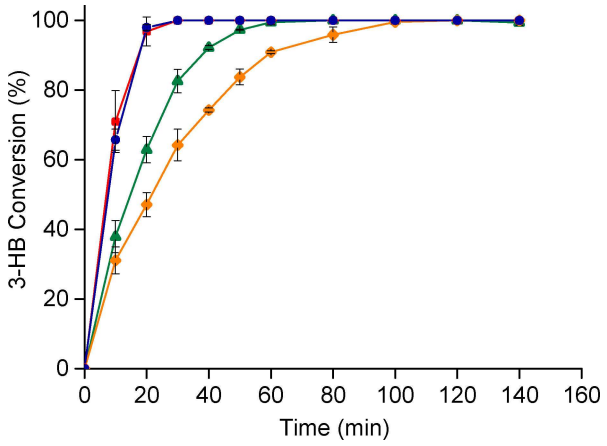

Figure 3. 3HB6H-catalyzed conversion of 3-HB to 2,5-DHB with: NADH (red squares), NADPH (blue circles), AmNAH (green triangles), BNAH (orange diamonds). Reaction conditions: 30 °C, 800 rpm; 1 mL total volume containing 2 μM 3HB6H, 5 mM 3-HB, 10 mM coenzyme and 50 mM Tris–SO_4 pH 8.0. Data points are an average of duplicates.

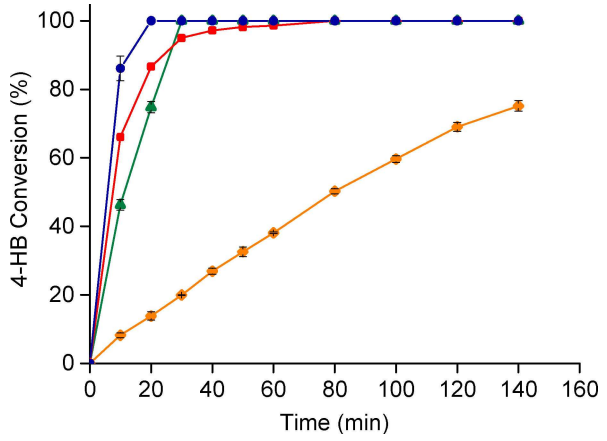

Figure 4. PHBH-catalyzed conversion of 4-HB to 3,4-DHB with: NADH (red squares), NADPH (blue circles), AmNAH (green triangles), BNAH (orange diamonds). Reaction conditions: 25 °C, 800 rpm; 1 mL total volume containing 4 μM PHBH, 5 mM 4-HB, 10 mM coenzyme and 50 mM Tris–SO_4 pH 8.0. Data points are an average of duplicates, with the exception of NADH.

benzoate, which contains an amino group instead of the typical hydroxyl substituent (Figure S2). In 48 h, 1 mM of the respective hydroxylated product 5-aminosalicylate was obtained.

Next, we monitored the hydroxylation of 4-hydroxybenzoate (4-HB, Figure 2B) catalyzed by PHBH with synthetic and natural coenzymes (Figure 4). Because of substrate inhibition (K_i for 4-HB of 8.5 mM),[27] we kept a substrate concentration of 5 mM. The preferred coenzyme NADPH showed the fastest conversion rates, with full conversion to 3,4-dihydroxybenzoate (3,4-DHB) in 20 min (Figure 4). The rate of product formation with AmNAH was similar to that with NADH: the initial conversion rate with AmNAH was somewhat lower than with NADH but full conversion was reached earlier with the carbamoylmethyl-substituted biomimetic. Using BNAH, 75% conversion was obtained after 140 min.

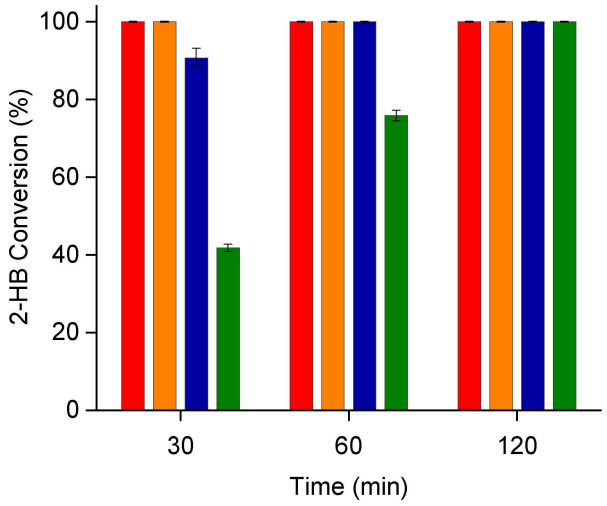

Figure 5. SalH-catalyzed conversion of 2-HB to catechol after 30, 60 and 120 min with: NADH (red), BNAH (orange), NADPH (blue) and AmNAH (green). Reaction conditions: 25 °C, 800 rpm; 1 mL total volume containing 3 μM SalH, 5 mM 2-HB, 10 mM coenzyme and 50 mM Tris–SO_4 pH 8.0. Data points are an average of duplicates (SI Table S4).

For SalH, the initial rate with BNAH was only 30% when compared with NADH (Figure S9). In contrast to 3HB6H and PHBH, SalH showed negligible activity with AmNAH (1.4% initial rate). The two synthetic coenzymes were compared with the natural ones for the oxidative decarboxylation of SalH's natural substrate salicylate (2-HB, Figure 2C and 5). In 30 min, full conversion to catechol was achieved with NADH and BNAH, whereas NADPH and AmNAH afforded 91% and 42% conversion, respectively. The poor initial rate measured for AmNAH is reflected in the time course of the biocatalytic reaction, with AmNAH being the last coenzyme to achieve full conversion (Figure 5).

BNAH, its acetyl-derivative BAPH, and AmNAH were tested with HbpA to convert 2-hydroxybiphenyl (2-HBP). The three synthetic coenzymes only gave conversions equal to or lower than 2% after 1 h (Figure 6). NADH and NADPH provided 2,3-dihydroxybiphenyl (2,3-DHB) in good conversions (84% and 76%, respectively, Figure 6). Considering that HbpA is inhibited by its substrate and product,[20] a set of experiments with varied concentrations of both BNAH and 2-HBP was designed (Figure 6, A–E). Low aromatic substrate concentrations were beneficial for the BNAH-mediated reaction of HbpA (Figure 6C–E). On the other hand, at a fixed concentration of 2-HBP, the concentration of the coenzyme itself seemed to have a negligible effect on the final conversion (C and D). Full conversion was obtained only at very low substrate concentrations (E), whereas, with 5 mM of substrate, meagre conversions ($\leq$2%) were achieved, independently of the equivalents of coenzyme present (A and B).

At a 2-HBP concentration of 0.1 mM, HbpA showed activity with all the tested NCBs (Table S3). As expected, NADH is the preferred coenzyme. Among the synthetic analogues, AmNAH showed the best result, retaining *ca.* 4% of the initial activity found for NADH.

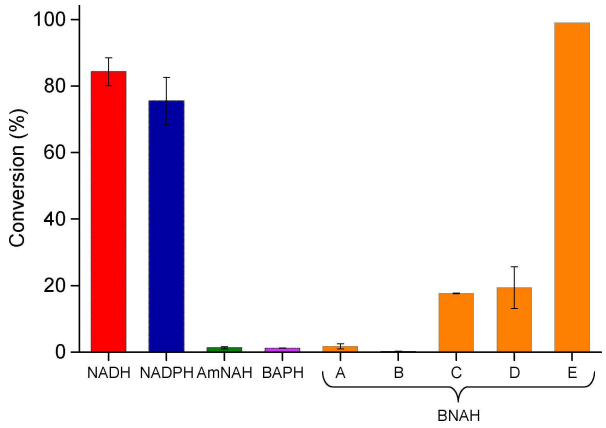

Figure 6. HbpA-catalyzed hydroxylation of 2-HBP with coenzymes, and at various BNAH and substrate concentrations (A–E). Reaction conditions: 30 °C, 800 rpm, 1 h; 1 mL total volume containing 2 μM HbpA, 50 mM NaPi pH 7.5 and 5% v/v DMSO, 5 mM 2-HBP (unless indicated otherwise), 10 mM coenzyme (unless indicated otherwise). **A**: 5 mM 2-HBP, 10 mM BNAH; **B**: 5 mM 2-HBP, 2 mM BNAH; **C**: 1 mM 2-HBP, 10 mM BNAH; **D**: 1 mM 2-HBP, 2 mM BNAH; **E**: 0.1 mM 2-HBP, 2 mM BNAH. Data are an average of duplicates (Table S2).

Kinetic parameters of hydroxylases with NCBs

To determine the reaction rates and catalytic efficiencies of the hydroxylases 3HB6H, PHBH and SalH with AmNAH and BNAH, we carried out steady-state kinetics under substrate-saturated conditions (Table 1). We observed that even at high concentration of the synthetic coenzymes, no plateau in the reaction rates was reached (SI section 2.6). Hence, only approximate k_{cat} and K_m values could be obtained for the NCBs.

The *para*-hydroxylase 3HB6H showed the lowest K_m and highest catalytic efficiency with NADH (Table 1, entry 1). In agreement with the results shown in Figure 3, the enzyme was also quite efficient with NADPH (Table 1, entry 2). The Michaelis constants calculated for the synthetic analogues are higher than 10 mM (Table 1, entry 3 and 4). As a result, both AmNAH and BNAH displayed far lower catalytic efficiencies with 3HB6H than with the natural coenzymes.

The *ortho*-hydroxylase PHBH exhibited a clear preference for NADPH with a high catalytic efficiency (Table 1, entry 6).[27] The estimated K_m constants of both NADH and AmNAH were two orders of magnitude higher than for NADPH (Table 1, entry 5 and 7). The catalytic efficiency of PHBH with AmNAH was in the same range as the one determined for NADH (Table 1, entry 5 and 7), in good agreement with the biocatalytic experiment (Figure 4).

The oxidative decarboxylase SalH showed a clear preference for NADH with a high catalytic efficiency of *ca.* 1430 $mM^{-1}s^{-1}$ (Table 1, entry 8). For NADPH and BNAH, no reliable k_{cat} values could be extrapolated from the obtained kinetic traces. Therefore, to compare the three coenzymes, the k_{cat} value obtained for NADH was used as a fixed value for the calculation of the Michaelis constant of NADPH and BNAH (Table 1, entry 9 and 10). Both K_m values estimated in this way were at least 100 times higher than the K_m value determined for NADH. On the other hand, AmNAH was hardly accepted by SalH (Figure 5 and S9).

Uncoupling rates in presence of NCBs

We monitored the activity of 3HB6H and PHBH in the presence of their respective product by measuring the rate of oxygen consumption either with NADH, NADPH or AmNAH (Table 2). Under those conditions, with the physiological electron donors, these enzymes can function as oxidases, leading to the

Table 1. Steady-state kinetic parameters of 3HB6H, PHBH and SalH for different coenzymes.

Entry	Enzyme	Coenzyme	K_m [mM]	k_{cat} [s^{-1}]	k_{cat}/K_m [$mM^{-1}s^{-1}$]
1	3HB6H[a]	NADH	0.06 ± 0.01	26.0 ± 0.8	429
2		NADPH	0.39 ± 0.08[c]	26[d]	66[d]
3		BNAH[b]	~10.6 ± 1.5	~3.4 ± 0.4	~0.32
4		AmNAH	~19.1 ± 4.4	~4.0 ± 0.7	~0.21
5	PHBH[e]	NADH	~4.7 ± 0.6	~4.3 ± 0.25	~0.91
6		NADPH[f]	0.07 ± 0.01	55.0 ± 0.6	786
7		AmNAH	~4.2 ± 0.4	~8.0 ± 0.3	~1.9
8	SalH[g]	NADH	0.009 ± 0.001	13.0 ± 0.3	1429
9		NADPH[h]	0.97 ± 0.12	13.0 ± 0.3	13.4
10		BNAH[h]	1.10 ± 0.17	13.0 ± 0.3	11.8

Kinetic constants were determined at 25 °C in 50 mM Tris–SO_4 pH 8.0. Results are an average of triplicates. [a] The final volume of 1 mL contained 1 mM 3-HB and varying coenzyme concentrations. [3HB6H] = 45 nM with NADH. [3HB6H] = 2.7 μM with synthetic coenzymes. [3HB6H] = 3.6 μM with [NCB] ≤ 150 μM. [b] with 5% v/v DMSO. [c] Literature value with 200 μM of 3-HB, 45 nM 3HB6H and 50 mM Tris–SO_4 pH 8.0.[17] [d] Previous unpublished results. [e] 200 μM 4-HB, 2 μM PHBH. [f] Literature value with 200 μM of 4-HB, 7.5 nM PHBH and 100 mM Tris–SO_4 pH 8.0.[27] [g] with 5% v/v DMSO, 1 mM 2-HB, 92 nM SalH, 10 μM FAD buffer. [h] The k_{cat} value obtained with NADH was used during the fitting of the kinetic traces obtained with NADPH and BNAH because of their high K_m values.

Table 2. Oxidase activities of free enzymes and enzyme-product complexes of 3HB6H and PHBH with NAD(P)H and AmNAH.

Entry	Enzyme	Coenzyme	[Coenzyme] [mM]	[Product] [mM]	k' [s^{-1}]
1	3HB6H[a]	NADH	0.25	0	0.045 ± 0.006
2				0.35	2.49 ± 0.15
3		AmNAH	1	0	0.014 ± 0.006
4			1	1	0.005 ± 0.002
5			8.4	0	0.004 ± 0.001
6			8.4	1	0.014 ± 0.001
7	PHBH[b]	NADPH	0.25	0	0.06 ± 0.01
8				1	2.34 ± 0.07
9		AmNAH	1	0	0.05 ± 0.03
10			1	1	0.06 ± 0.02
11			8	1	0.45 ± 0.05
12		NADH	1	0	0.04 ± 0.05
13			1	1	0.02 ± 0.01
14			8	0	0.03 ± 0.01
15			8	1	0.07 ± 0.04

Apparent reaction rates (k') were determined with a Clarke-type electrode at 25 °C in 50 mM Tris–SO_4 pH 8.0. The final volume of 1 mL contained the specified concentrations of coenzyme and product (2,5-DHB for 3HB6H and 3,4-DHB for PHBH). [a] [3HB6H] = 1 μM with NADH. [3HB6H] = 2.7 μM with AmNAH, [b] [PHBH] = 1 μM with NADPH. [PHBH] = 2 μM with AmNAH and NADH. Results are an average of triplicates.

production of hydrogen peroxide (H_2O_2), known as the uncoupling reaction.[17,28]

In the presence of its product 2,5-DHB and NADH, 3HB6H increased its oxygen consumption due to H_2O_2 generation, giving an uncoupling rate of 2.49 s^{-1} (Table 2, entry 2), whereas high concentrations of AmNAH provided an apparent rate of only 0.014 s^{-1}, independently of the presence or absence of product (Table 2, entry 3 and 4). Overall, similar results were observed with PHBH. Its product 3,4-DHB and NADPH gave an apparent rate 40 times higher than in absence of 3,4-DHB (Table 2, entry 7 and 8).[29] With 1 mM of AmNAH, the presence of one equivalent of 3,4-DHB did not stimulate the uncoupling reaction (Table 2, entry 9 and 10). An eight times higher concentration of AmNAH gave a slightly higher uncoupling rate (Table 2, entry 11). For the reaction of PHBH and NADH, the presence of 8 mM of NADH hardly increased the reaction rate (Table 2, entry 12, 13 and 14).

Activity of Type I BVMOs with NCBs

In the interest of our study, we performed a screening with group B flavoprotein monooxygenases Type I BVMOs for the selective oxidation of two substrates with BNAH. However, we observed no conversion with the purified wild type CHMO, mutant $CHMO_{M16}$,[24] and $BVMO_{791}$[25] (SI section 2.7).

Discussion

NCBs are used in redox biocatalysis as alternatives to NAD(P)(H) and were recently reviewed.[8,30] In this study, we investigated the applicability of NCBs (Figure 1) for the enzymatic regioselective hydroxylation of aromatic compounds with several flavoenzymes (Figure 2). Moreover, we compared the kinetic capabilities of these NCBs to those of natural coenzymes, also in terms of electron efficiency. The chosen biocatalysts 3HB6H, PHBH, SalH and HbpA follow a reaction cycle similar to the one depicted in Figure 7 for PHBH.[18,31] In the reductive part of the reaction cycle, the aromatic substrate acts as an effector (Figure 7, I), strongly enhancing the rate of flavin reduction by NAD(P)H (Figure 7, II).[32] The intimate link between NAD(P)H oxidation and substrate binding decreases the risk that the labile C4a-hydroperoxide intermediate ($FADH_{OOH}$) decomposes, thereby generating H_2O_2 (*vide infra*).

For decades, the way flavin and pyridine nucleotide coenzymes approach each other for hydride transfer in group A enzymes was unclear.[33] Crystallographic studies revealed that the isoalloxazine moiety of the FAD cofactor of PHBH is able to swing out of the active site.[34] Based on these observations, PHBH would bind NADPH through a conformational selection mechanism and flavin reduction would take place in the exposed flavin *out* conformation (Figure 8).[18,32a,b,34a,35] After $NADP^+$ release, the anionic reduced flavin swings back into the buried active site, where the subsequent reactions with oxygen occur. Other group A flavoproteins monooxygenases are assumed to display a similar mechanism.[3c,36] Data indicates that

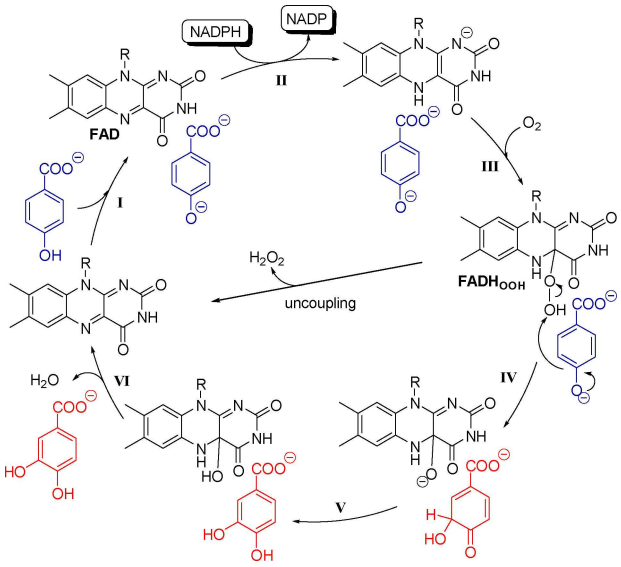

Figure 7. Schematic representation of the proposed catalytic cycle for the PHBH-mediated hydroxylation of 4-HB to 3,4-DHB and the uncoupling reaction *via* $FADH_{OOH}$ leading to H_2O_2 production.

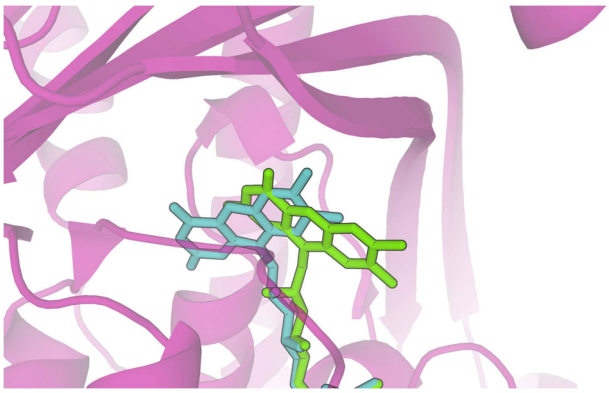

Figure 8. FAD cofactor in the active site of PHBH in the *in* (cyan, PDB ID: 1PBE) and *out* (green, PDB ID: 1PDH) conformation.

HbpA also adopts the *in-out* FAD movement during catalysis,[18,36b] whereas these conformational changes for 3HB6H and SalH remain unexplored.

In the oxidative part of the catalytic cycle, the reaction of reduced flavin with molecular oxygen generates $FADH_{OOH}$ (Figure 7, III). This electrophilic oxygenation species reacts with the aromatic substrate, yielding the dihydroxylated aromatic product (Figure 7, IV and V). The efficiency of substrate hydroxylation is enzyme and substrate dependent and relates to the stability and reactivity of $FADH_{OOH}$ and the activation of the substrate.[18,31,32d,37] In the absence of substrate or in the presence of the aromatic product (which serves as a non-substrate effector), the enzyme may act as an NAD(P)H oxidase, generating H_2O_2,[17,22b,28,32d] a reactive oxygen species detrimental to the enzyme and resulting in a loss of precious electrons.

Biocatalytic reactions with NCBs

The biocatalytic experiments performed in this study establish that NCBs can successfully replace the natural pyridine nucleotide coenzyme in group A flavoenzyme-mediated hydroxylation reactions. Especially with 3HB6H, PHBH and SalH, full substrate conversions were obtained within a reasonably short time frame (Figure 3, 4 and 5). The steady-state kinetic studies indicate that absence of a specific interaction with the adenine dinucleotide moiety of the coenzyme causes weak NCB binding and relatively low turnover rates (Table 1). In spite of this, there is a difference in the acceptance of NCBs among the enzymes. 3HB6H and PHBH both accept AmNAH as NCB (Figure 2 and 3), whereas SalH prefers BNAH (Figure 5). BCNPH provides no conversion, which can be ascribed to the lack of a carbonyl group in its structure, as seen with ene reductase-catalyzed reactions.[10a]

Electron efficiency of flavoenzyme-mediated hydroxylations with NCBs

The efficient substrate conversion observed with 3HB6H and PHBH in case of the water-soluble AmNAH (Figure 3 and 4) prompted us to have a closer look at the oxidase activity of these enzymes. This investigation revealed that in the presence of AmNAH, the aromatic products of these enzymes do not stimulate the formation of H_2O_2, and thus no longer act as effectors (Table 2). This provides an advantage for the biocatalytic reactions because with increasing product concentrations, no uncoupling, and thus no wasteful consumption of the electron donor takes place.

As explained above, the reductive step of the reaction depends on the prior association of the nicotinamide coenzyme to the enzyme-substrate complex (Figure 7). Only when the proper ternary complex is achieved, flavin reduction takes place.[32b] With 3HB6H[32e] and PHBH,[38] reduction of the enzyme-substrate complex with the natural electron donor is faster than the reaction turnover rate. With the NCBs, however, assuming these compounds do not interfere with the oxidative half-reaction, flavin reduction becomes rate limiting in overall catalysis (Table 1 and 2). This is in line with the idea that rapid flavin reduction requires enhanced sampling of the donor-acceptor distance (conformational selection), which in group A monooxygenases is tightly regulated by substrate binding and achieved by orienting the nicotinamide ring of NAD(P)H in close proximity to the exposed isoalloxazine ring of FAD.[7] We therefore introduce the term 'kiss and ride' mechanism. The weak binding of the NCBs reduces the chance that the isoalloxazine and nicotinamide rings meet each other for a 'kiss', but as soon as this happens, the reaction will proceed ('ride'). In the case of product binding, the optimal orientation between flavin and NCBs that leads to reduction (the 'kiss') is no longer achieved.

Replacing NAD(P)H with NCBs: challenges and prospects

So far, NCBs have been applied in stoichiometric amounts to biocatalytic reactions. An efficient recycling system, whether chemically with transition metals,[39] or enzymatically with a dehydrogenase enzyme,[9c,30,40] is still limited by turnover numbers lower than a few hundred, but will hopefully be overcome by new computational modeling and protein engineering approaches in the near future.[40]

Additionally, as differently substituted NCBs can lead to variable stability and redox potential as well as enzyme specificity, the type of NCB should match the enzyme desired to catalyze a reaction. Regarding SalH, we observed this enzyme accepts BNAH as the best mimic, while 3HB6H and PHBH are more efficient with AmNAH. Subtle conformational fluctuations near the domain interface[7,35,38,41] are expected to also play a role, as PHBH accepts NADPH better than NADH (Figure 4; Table 1).

The stable biomimetic AmNAH is accepted as a coenzyme in the 3HB6H-catalyzed reaction to achieve a 10 mM/h conversion to gentisate (Figure 2A), which has interesting anti-inflammatory and anti-bacterial activity.[5] Using this system, we also produce 5-aminosalicylate (mesalazine, used to treat inflammatory pathologies[42]) from 3-aminobenzoate. Nevertheless, further optimization is needed to use AmNAH efficiently with a recycling system.

The tested NCBs show conversions lower or equal to 2% with HbpA on a 5 mM reaction scale, compared with good conversions when using NADH or NADPH. HbpA unfortunately suffers from substrate (K_i 2-HBP of 6.5 mM) and product inhibition (K_i 2,3-DHBP of 0.9 mM),[20] which would explain our low conversions. Our presented panel of coenzyme analogues is of a small sample size, and other dihydropyridines might afford better activity. Mutagenesis[43] could be considered to enhance HbpA's affinity towards NCBs.[44]

Finally, in an attempt to further explore the potential of NCBs with flavoprotein monooxygenases, we investigated FAD-containing Type I BVMOs to establish their activity towards NCBs, essentially BNAH, catalysing the oxygenation of cyclohexanone to caprolactone and asymmetric sulfoxidation. The purified BVMOs displayed no observable activity with BNAH (Table S8). Unlike the flavin-containing group A monooxygenases, group B enzymes present a Rossmann fold that binds the NAD(P)H dinucleotide moiety throughout the entire catalytic cycle.[45] As demonstrated here, this feature makes NCBs unable to function as electron donors of Type I BVMOs. Thus, group B flavoprotein monooxygenases, usually regarded as being 'bold' in terms of flavin reduction, are more critical with NCBs than group A enzymes, which usually are referred to as being 'cautious'.[23,46]

Conclusions

We show the proof of principle that group A flavoprotein hydroxylases can use coenzyme biomimetics for different regioselective hydroxylation reactions on both phenolic and

biphenolic substrates, enabling full conversions. NCBs showed different catalytic efficiencies depending on the hydroxylase enzyme: these results highlight the importance of selecting the best synthetic coenzyme for each monooxygenase. Moreover, for biocatalytic purposes, the application of NCBs can be enlarged by improving substrate and product inhibition, as in the case for HbpA.

Overall, NCBs revealed higher K_m and lower k_{cat} values, supporting the view that the enzyme-NCB complexes are more disordered than the natural enzyme-coenzyme complexes. Intriguingly, the NCB-mediated biocatalytic conversions displayed less uncoupling than the biocatalytic reactions with the natural coenzymes. This represents an advantage since the electron transfer efficiency of the reaction is improved and the H_2O_2 formation, detrimental for the enzyme and unnecessarily consuming precious electrons, is reduced. Mechanistic and biocatalytic details on the production of hydroxylated aromatic compounds of medicinal interest were discussed and applied, resulting in the potential future exploitation of NCBs for other or improved hydroxylase-catalyzed reactions towards the regioselective oxidation of aromatic compounds or the recently applied oxidative dearomatization.[47]

Experimental Section

General information: All chemicals were purchased from Sigma-Aldrich (Merck) or Alfa Aesar and were used without further purification unless otherwise specified. The natural nicotinamide adenine dinucleotide coenzymes, both oxidized and reduced, were purchased from Prozomix. ^{1}H and ^{13}C NMR spectra were recorded on a Varian 400 or a Bruker Avance III 400 NMR spectrometer at 400 or 100 MHz, respectively, internally referenced to residual proton signals in $CDCl_3$, D_2O or DMSO-d_6. HPLC analyses were carried out at 30 °C on an Agilent Technologies UHPLC 1290 Infinity System with a ZORBAX Eclipse XDB-C18 column (Agilent, 3.0×250 mm×5 μm). GC analyses were carried out on a Hewlett Packard HP6890 GC system connected to a DB-5MS capillary column (Agilent, 30 m×0.25 mm×0.25 μm). UV-Vis spectra were recorded on a UV/visible-spectrophotometer Ultrospec 2000, connected to a temperature control unit, both from Amersham Pharmacia Biotech. Oxygen consumption experiments were carried out with a Clarke-type electrode system (Hansatech Oxytherm).

Production of enzymes: 3-Hydroxybenzoate 6-hydroxylase from *Rhodococcus jostii* RHA1 (3HB6H), *p*-hydroxybenzoate hydroxylase Cys116Ser variant from *Pseudomonas fluorescens* (PHBH) and 2-hydroxybiphenyl 3-hydroxylase from *Pseudomonas azelaica* HBP1 (HbpA) were produced from recombinant expression in *Escherichia coli* and purified as described previously.[17,27,32d] Salicylate hydroxylase from *Pseudomonas putida* S-1 was purified as described by Yamamoto *et al.*[19] Enzyme concentrations were determined by measuring the absorbance for protein-bound FAD using the following molar absorption coefficients: 3HB6H, ε_{453} = 10300 $M^{-1}cm^{-1}$;[17] PHBH, ε_{453} = 10200 $M^{-1}cm^{-1}$;[27] HbpA, ε_{452} = 9700 $M^{-1}cm^{-1}$;[32d] SalH, ε_{450} = 11300 $M^{-1}cm^{-1}$.[19]

Example of biocatalytic hydroxylation reactions with 3HB6H: The coenzyme (2 equiv., 10 mM) was weighed in a 2 mL Eppendorf microcentrifuge plastic tube (NADH: 7.1 mg; NADPH: 8.3 mg; AmNAH: 1.8 mg; BNAH: 2.1 mg). 50 mM Tris–SO_4 pH 8.0 buffer, 5 mM of substrate (3-HB, 1 equiv., from a 10 mM stock in buffer) and 3HB6H (2 μM) were added to reach 1 mL total reaction volume. The reactions were carried out in duplicate at 30 °C and 800 revolutions per minute (rpm) for 2 h 20 min with an Eppendorf Thermomixer C. Aliquots to monitor the reaction over time were quenched with a mixture of acetonitrile and milliQ water (1:1.75). Prior to HPLC injection, the samples were filtered through an Amicon Ultra-0.5 mL centrifugal filter units with Ultracel-10 membranes.

Example of kinetic data for 3HB6H: All measurements were performed in triplicates at 25 °C in 50 mM Tris–SO_4 pH 8.0 in a final volume of 1.0 mL. Steady-state kinetics were measured under substrate saturation conditions with varying coenzyme concentrations. Data was fitted to the Michaelis-Menten equation (OriginPro version 9.0). Reactions with NADH contained 1.0 mM 3-HB, 45 nM 3HB6H, 50 mM Tris–SO_4 pH 8.0 and varying coenzyme concentrations (0–250 μM), either in presence or in absence of 5% v/v DMSO. The enzyme reactions were monitored by UV/visible-spectrophotometry, following the decrease in absorbance of NADH at 360 nm. Initial rates were determined using a molar absorption coefficient of 4.31 $mM^{-1}cm^{-1}$.

More information relating to the synthesis of coenzymes and NMR characterization, biocatalytic reactions, kinetic data and other details, can be found in the supporting information.

Acknowledgements

This project has received funding from the European Union's Horizon 2020 MSCA ITN-EJD program under grant agreement No 764920. AG, CEP and WJHB are grateful to the VLAG graduate school at Wageningen University. CEP acknowledges a Netherlands Organization for Scientific Research VENI grant (No 722.015.011). The authors thank M. van Schie for a preliminary kinetic assay with 3HB6H, Dr. C. Tolmie and E. Schuiten for preliminary screenings of BVMOs, and E. van der Klift, M. Strampraad and S. Eustace for technical assistance.

Conflict of Interest

The authors declare no conflict of interest.

Keywords: coenzyme specificity · flavin-containing monooxygenases · hydroxylases · nicotinamide coenzyme biomimetics · selective oxidation

[1] a) A. E. Shilov, G. B. Shul'pin, *Chem. Rev.* **1997**, *97*, 2879–2932; b) D. A. Alonso, C. Nájera, I. M. Pastor, M. Yus, *Chem. Eur. J.* **2010**, *16*, 5274–5284.
[2] E. Churakova, M. Kluge, R. Ullrich, I. Arends, M. Hofrichter, F. Hollmann, *Angew. Chem. Int. Ed.* **2011**, *50*, 10716–10719; *Angew. Chem.* **2011**, *123*, 10904–10907.
[3] a) E. Romero, J. R. G. Castellanos, G. Gadda, M. W. Fraaije, A. Mattevi, *Chem. Rev.* **2018**, *118*, 1742–1769; b) J. J. Dong, E. Fernández-Fueyo, F. Hollmann, C. E. Paul, M. Pesic, S. Schmidt, Y. H. Wang, S. Younes, W. Y. Zhang, *Angew. Chem. Int. Ed.* **2018**, *57*, 9238–9261; c) M. M. E. Huijbers, S. Montersino, A. H. Westphal, D. Tischler, W. J. H. van Berkel, *Arch. Biochem. Biophys.* **2014**, *544*, 2–17.
[4] V. Massey, *J. Biol. Chem.* **1994**, *269*, 22459–22462.
[5] R. S. Borges, S. L. Castle, *Bioorg. Med. Chem. Lett.* **2015**, *25*, 4808–4811.
[6] W. J. H. van Berkel, N. M. Kamerbeek, M. W. Fraaije, *J. Biotechnol.* **2006**, *124*, 670–689.

[7] A. H. Westphal, D. Tischler, F. Heinke, S. Hofmann, J. A. D. Groning, D. Labudde, W. J. H. van Berkel, *Front. Microbiol.* **2018**, *9*, Article 3050.
[8] a) C. E. Paul, I. W. C. E. Arends, F. Hollmann, *ACS Catal.* **2014**, *4*, 788–797; b) F. Hollmann, C. E. Paul, *BIOspektrum* **2015**, *21*, 376–378; c) C. E. Paul, F. Hollmann, *Appl. Microbiol. Biotechnol.* **2016**, *100*, 4773–4778; d) A. Guarneri, W. J. H. van Berkel, C. E. Paul, *Curr. Opin. Biotechnol.* **2019**, *60*, 63–71.
[9] a) J. B. Jones, K. E. Taylor, *Can. J. Chem.* **1976**, *54*, 2974–2980; b) H. C. Lo, R. H. Fish, *Angew. Chem. Int. Ed.* **2002**, *41*, 478–481; *Angew. Chem.* **2002**, *114*, 496–499; c) C. Nowak, A. Pick, P. Lommes, V. Sieber, *ACS Catal.* **2017**, *7*, 5202–5208; d) L. Josa-Culleré, A. S. K. Lahdenperä, A. Ribaucourt, G. T. Höfler, S. Gargiulo, Y.-Y. Liu, J.-H. Xu, J. Cassidy, F. Paradisi, D. J. Opperman, F. Hollmann, C. E. Paul, *Catalysts* **2019**, *9*, Article 207.
[10] a) C. E. Paul, S. Gargiulo, D. J. Opperman, I. Lavandera, V. Gotor-Fernández, V. Gotor, A. Taglieber, I. W. C. E. Arends, F. Hollmann, *Org. Lett.* **2013**, *15*, 180–183; b) T. Knaus, C. E. Paul, C. W. Levy, S. de Vries, F. G. Mutti, F. Hollmann, N. S. Scrutton, *J. Am. Chem. Soc.* **2016**, *138*, 1033–1039; c) S. A. Löw, I. M. Löw, M. J. Weissenborn, B. Hauer, *ChemCatChem* **2016**, *8*, 911–915; d) A. Scholtissek, D. Tischler, A. H. Westphal, W. J. H. van Berkel, C. E. Paul, *Catalysts* **2017**, *7*, Article 130; e) A. Scholtissek, E. Gadke, C. E. Paul, A. H. Westphal, W. J. H. van Berkel, D. Tischler, *Front. Microbiol.* **2018**, *9*, Article 2410.
[11] J. X. Qi, C. E. Paul, F. Hollmann, D. Tischler, *Enzyme Microb. Technol.* **2017**, *100*, 17–19.
[12] a) J. D. Ryan, R. H. Fish, D. S. Clark, *ChemBioChem* **2008**, *9*, 2579–2582; b) C. E. Paul, E. Churakova, E. Maurits, M. Girhard, V. B. Urlacher, F. Hollmann, *Bioorg. Med. Chem.* **2014**, *22*, 5692–5696.
[13] C. Nowak, B. Beer, A. Pick, T. Roth, P. Lommes, V. Sieber, *Front. Microbiol.* **2015**, *6*, Article 957.
[14] a) C. E. Paul, D. Tischler, A. Riedel, T. Heine, N. Itoh, F. Hollmann, *ACS Catal.* **2015**, *5*, 2961–2965; b) M. Ismail, L. Schroeder, M. Frese, T. Kottke, F. Hollmann, C. E. Paul, N. Sewald, *ACS Catal.* **2019**, *9*, 1389–1395.
[15] J. A. Rollin, T. K. Tam, Y.-H. P. Zhang, *Green Chem.* **2013**, *15*, 1708–1719.
[16] A. Geddes, C. E. Paul, S. Hay, F. Hollmann, N. S. Scrutton, *J. Am. Chem. Soc.* **2016**, *138*, 11089–11092.
[17] S. Montersino, W. J. H. van Berkel, *BBA Proteins Proteom.* **2012**, *1824*, 433–442.
[18] B. Entsch, W. J. H. van Berkel, *FASEB J.* **1995**, *9*, 476–483.
[19] S. Yamamoto, M. Katagiri, H. Maeno, O. Hayaishi, *J. Biol. Chem.* **1965**, *240*, 3408–3413.
[20] W. A. Suske, M. Held, A. Schmid, T. Fleischmann, M. G. Wubbolts, H. P. E. Kohler, *J. Biol. Chem.* **1997**, *272*, 24257–24265.
[21] S. Montersino, D. Tischler, G. T. Gassner, W. J. H. van Berkel, *Adv. Synth. Catal.* **2011**, *353*, 2301–2319.
[22] a) M. Held, W. Suske, A. Schmid, K. H. Engesser, H. P. E. Kohler, B. Witholt, M. G. Wubbolts, *J. Mol. Catal. B: Enzym.* **1998**, *5*, 87–93; b) R. H. White-Stevens, H. Kamin, *J. Biol. Chem.* **1972**, *247*, 2358–2370.
[23] M. J. L. J. Fürst, F. Fiorentini, M. W. Fraaije, *Curr. Opin. Struct. Biol.* **2019**, *59*, 29–37.
[24] D. J. Opperman, M. T. Reetz, *ChemBioChem* **2010**, *11*, 2589–2596.
[25] F. M. Ferroni, C. Tolmie, M. S. Smit, D. J. Opperman, *ChemBioChem* **2017**, *18*, 515–517.
[26] a) R. J. Knox, T. C. Jenkins, S. M. Hobbs, S. A. Chen, R. G. Melton, P. J. Burke, *Cancer Res.* **2000**, *60*, 4179–4186; b) C. Nowak, A. Pick, L. I. Csepei, V. Sieber, *ChemBioChem* **2017**, *18*, 1944–1949.
[27] W. J. H. van Berkel, A. Westphal, K. Eschrich, M. Eppink, A. de Kok, *Eur. J. Biochem.* **1992**, *210*, 411–419.
[28] T. Spector, V. Massey, *J. Biol. Chem.* **1972**, *247*, 4679–4687.
[29] K. Eschrich, F. J. van der Bolt, A. de Kok, W. J. van Berkel, *Eur. J. Biochem.* **1993**, *216*, 137–146.
[30] I. Zachos, C. Nowak, V. Sieber, *Curr. Opin. Chem. Biol.* **2018**, *49*, 59–66.
[31] B. Entsch, D. P. Ballou, V. Massey, *J. Biol. Chem.* **1976**, *251*, 2550–2563.
[32] a) D. P. Ballou, B. Entsch, *Handbook of Flavoproteins: Complex Flavoproteins, Dehydrogenases and Physical Methods, Vol 2* **2013**, 1–28; b) B. A. Palfey, G. R. Moran, B. Entsch, D. P. Ballou, V. Massey, *Biochemistry* **1999**, *38*, 1153–1158; c) L. G. Howell, T. Spector, V. Massey, *J. Biol. Chem.* **1972**, *247*, 4340–4350; d) W. A. Suske, W. J. H. van Berkel, H. P. E. Kohler, *J. Biol. Chem.* **1999**, *274*, 33355–33365; e) J. Sucharitakul, T. Wongnate, S. Montersino, W. J. H. van Berkel, P. Chaiyen, *Biochemistry* **2012**, *51*, 4309–4321; f) M. Husain, V. Massey, *J. Biol. Chem.* **1979**, *254*, 6657–6666.
[33] H. A. Schreuder, P. A. J. Prick, R. K. Wierenga, G. Vriend, K. S. Wilson, W. G. J. Hol, J. Drenth, *J. Mol. Biol.* **1989**, *208*, 679–696.
[34] a) W. J. H. van Berkel, M. H. M. Eppink, H. A. Schreuder, *Protein Sci.* **1994**, *3*, 2245–2253; b) H. A. Schreuder, A. Mattevi, G. Obmolova, K. H. Kalk, W. G. J. Hol, F. J. T. van der Bolt, W. J. H. van Berkel, *Biochemistry* **1994**, *33*, 10161–10170; c) D. L. Gatti, B. A. Palfey, M. S. Lah, B. Entsch, V. Massey, D. P. Ballou, M. L. Ludwig, *Science* **1994**, *266*, 110–114.
[35] J. Wang, M. Ortiz-Maldonado, B. Entsch, V. Massey, D. Ballou, D. L. Gatti, *Proc. Natl. Acad. Sci.* **2002**, *99*, 608–613.
[36] a) T. Hiromoto, S. Fujiwara, K. Hosokawa, H. Yamaguchi, *J. Mol. Biol.* **2006**, *364*, 878–896; b) M. Kanteev, A. Bregman-Cohen, B. Deri, A. Shahar, N. Adir, A. Fishman, *BBA Proteins Proteom.* **2015**, *1854*, 1906–1913.
[37] a) J. Sucharitakul, D. Medhanavyn, D. Pakotiprapha, W. J. H. van Berkel, P. Chaiyen, *FEBS J.* **2016**, *283*, 860–881; b) J. Sucharitakul, C. Tongsook, D. Pakotiprapha, W. J. H. van Berkel, P. Chaiyen, *J. Biol. Chem.* **2013**, *288*, 35210–35221.
[38] M. H. M. Eppink, H. A. Schreuder, W. J. H. van Berkel, *J. Biol. Chem.* **1998**, *273*, 21031–21039.
[39] a) Y. Okamoto, V. Kohler, C. E. Paul, F. Hollmann, T. R. Ward, *ACS Catal.* **2016**, *6*, 3553–3557; b) J. Kim, S. H. Lee, F. Tieves, D. S. Choi, F. Hollmann, C. E. Paul, C. B. Park, *Angew. Chem. Int. Ed.* **2018**, *57*, 13825–13828.
[40] R. Huang, H. Chen, D. M. Upp, J. C. Lewis, Y.-H. P. J. Zhang, *ACS Catal.* **2019**, *9*, 11709–11719.
[41] M. H. M. Eppink, K. M. Overkamp, H. A. Schreuder, W. J. H. van Berkel, *J. Mol. Biol.* **1999**, *292*, 87–96.
[42] S. B. Hanauer, *Aliment. Pharmacol. Ther.* **2004**, *20*, 60–65.
[43] A. Meyer, A. Schmid, M. Held, A. H. Westphal, M. Rothlisberger, H. P. E. Kohler, W. J. H. van Berkel, B. Witholt, *J. Biol. Chem.* **2002**, *277*, 5575–5582.
[44] C. N. Jensen, T. Mielke, J. E. Farrugia, A. Frank, H. Man, S. Hart, J. P. Turkenburg, G. Grogan, *ChemBioChem* **2015**, *16*, 968–976.
[45] R. Orru, H. M. Dudek, C. Martinoli, D. E. T. Pazmino, A. Royant, M. Weik, M. W. Fraaije, A. Mattevi, *J. Biol. Chem.* **2011**, *286*, 29284–29291.
[46] a) B. A. Palfey, C. A. McDonald, *Arch. Biochem. Biophys.* **2010**, *493*, 26–36; b) J. W. Setser, J. R. Heemstra, C. T. Walsh, C. L. Drennan, *Biochemistry* **2014**, *53*, 6063–6077.
[47] a) S. A. B. Dockrey, A. L. Lukowski, M. R. Becker, A. R. H. Narayan, *Nat. Chem.* **2018**, *10*, 119–125; b) A. Abood, A. Al-Fahad, A. Scott, A. E. D. M. S. Hosny, A. M. Hashem, A. M. A. Fattah, P. R. Race, T. J. Simpson, R. J. Cox, *RSC Adv.* **2015**, *5*, 49987–49995.

Manuscript received: October 29, 2019
Revised manuscript received: December 16, 2019
Accepted manuscript online: December 17, 2019
Version of record online: January 23, 2020